Polymer Bulletin (2026) 83:226
https://doi.org/10.1007/s00289-025-06276-3

ORIGINAL PAPER

In situ synthesis and functional properties of poly(butyl methacrylate)/Na-montmorillonite composites

Pınar Acar Bozkurt[1] · Sibel Erol Dağ[2] · Meltem Çelik[1] · Süheyla Pınar Çelik[3] · Leyla Açık[3]

Received: 24 August 2025 / Revised: 29 November 2025 / Accepted: 28 December 2025
© The Author(s) 2026

Abstract

Poly(butyl methacrylate) (PBMA)/sodium montmorillonite (Na-MMT) composites were successfully synthesized via in situ free-radical polymerization using benzoyl peroxide as an initiator to examine the influence of *unmodified* clay layers on the structural, thermal, and functional properties within the composites. The resulting composites were comprehensively characterized by Fourier-transform infrared spectroscopy (FTIR), X-ray diffraction (XRD), thermogravimetric analysis (TGA), scanning and transmission electron microscopy (SEM, TEM), and Brunauer–Emmett–Teller (BET) surface area analysis. TGA results indicated that the incorporation of Na-MMT promoted an intercalated morphology and the formation of a compact, thermally stable hybrid network. XRD and SEM analyses confirmed an increase in interlayer spacing and significant changes in surface morphology, evidencing effective monomer intercalation into the clay galleries. The addition of Na-MMT notably reduced water uptake and moisture retention efficiency, generated a tunable micro-/mesoporous structure, reflecting the strong reinforcing effect of the *unmodified* clay. Furthermore, the PBMA/Na-MMT composites exhibited superior antibacterial activity compared to pure PBMA, demonstrating synergistic polymer–clay interactions. Overall, this study establishes in situ organo–inorganic hybridization as an efficient strategy for developing multifunctional PBMA–clay materials with enhanced structural, thermal, and antibacterial properties, suitable for potential applications in packaging, coatings, and antimicrobial surfaces.

Keywords Composite · Sodium montmorillonite · Poly(butyl methacrylate) · Benzoyl peroxide · In situ polymerization

Extended author information available on the last page of the article

Published online: 19 January 2026

Introduction

Over the past two decades, polymer/clay composites have attracted considerable attention due to their substantial enhancements in physical, optical, and mechanical properties compared to neat polymers and conventional composites in engineering applications [1–11]. Even at low clay loadings, these composites exhibit notable improvements, particularly in mechanical, thermal, and antibacterial properties. The antibacterial functionality of polymer/clay composites is of particular interest for biomedical applications, positioning these materials as a promising new class of functional biomaterials [4]. Polymer/clay-based antimicrobial coatings are known for providing long-lasting protection against a wide range of microorganisms, including bacteria, fungi, and, in some cases, viruses. Such coatings are extensively applied to sterilize medical devices and surfaces, significantly reducing the risk of healthcare-associated infections. Moreover, their utility has expanded into diverse sectors, including food processing and packaging, aerospace, interior design, glass manufacturing, and HVAC (Heating, Ventilating, and Air Conditioning) systems, where they help maintain hygiene and prevent contamination on high-contact surfaces.

Among various layered silicates, sodium montmorillonite (Na-MMT) is one of the most commonly employed inorganic fillers, particularly in the plastics industry. Its unique TOT (tetrahedral–octahedral–tetrahedral) crystal structure, consisting of two tetrahedral silica layers sandwiching an octahedral alumina layer, combined with its abundance, low cost, non-toxicity, and excellent chemical and thermal stability, makes it highly suitable for polymer/clay nanocomposite fabrication [12]. As a layered silicate, Na-MMT not only reduces polymer crystallinity but also enhances mechanical and thermal properties, while providing high surface area, intercalation, and exfoliation capabilities.

Poly(butyl methacrylate) (PBMA) is a hydrophobic polymer with a low glass-transition temperature, widely used in the plastics industry. Its optical transparency and mechanical properties make it an attractive polymer matrix for the synthesis of diverse composites [12, 13], and it is also utilized in coatings and biomedical materials. However, the inherent thermal stability, mechanical performance, and antibacterial functionality of PBMA often remain inadequate, necessitating reinforcement strategies. Incorporating clays as inorganic fillers via in situ polymerization has been shown to improve these properties. The presence of clay layers promotes better dispersion within the polymer matrix, reduces heat transfer, and enhances thermal stability [14]. Accordingly, this study aims to improve the thermal, mechanical, and antibacterial properties of PBMA through its in situ polymerization with *unmodified* Na-MMT.

A review of the literature indicates that although numerous studies have investigated polymer/clay composites, reports on the use of *unmodified* montmorillonite as a filler remain limited. Therefore, the present work focuses on the in situ free radical polymerization of butyl methacrylate with *unmodified* Na-MMT at varying BMA loadings. The resulting composites are thoroughly characterized, with detailed investigations of moisture retention, water uptake, antibacterial activity, and thermal properties. This study distinguishes itself by focusing on the innovative aspects and positive contributions of the synthesized composites, rather than the limitations com-

monly emphasized in comparative research. The originality of this work is clearly demonstrated through its unique features and environmentally sustainable methodology, which eliminates the need for surface-modified clays or complex processing steps. Furthermore, the composites developed herein exhibit distinct structural and functional improvements imparted by *unmodified* Na-MMT, underscoring the novelty and scientific significance of this approach compared to previously reported materials.

Materials and methods

Materials

The Na-Montmorillonite (Na-MMT) clay used in this study was obtained from bentonite reserves located in Reşadiye (Tokat, Turkey) and was oven-dried before application. Exhibiting a cation exchange capacity (CEC) of 108 meq/100 g, the clay was subjected to further purification processes prior to use [15]. Its specific surface area was determined to be 67.56 m^2/g, while X-ray diffraction (XRD) analysis revealed an interlayer spacing of 1.18 nm. For composite synthesis, Na-MMT was utilized in its raw, unmodified state. Benzoyl peroxide (Bz_2O_2, Merck), serving as the free radical initiator, was purified by recrystallization using a methanol–chloroform solvent system. The butyl methacrylate (BMA, Merck) monomer was purified via vacuum distillation to remove any polymerization inhibitors. Bacterial strains employed in the experimental procedures were obtained from the Department of Biology at Gazi University (Ankara, Turkey). All other reagents and chemicals were used as received, without additional purification unless specifically noted.

Methods

Synthesis of PBMA/Na-MMT composites

Poly(butyl methacrylate) (PBMA) composites incorporating *unmodified* Na-montmorillonite (Na-MMT) were synthesized through in situ polymerization in aqueous media, following modified procedures from previous studies [4, 16]. To begin, 1 g of Na-MMT was uniformly dispersed in 24 mL of distilled water by magnetic stirring at 100 rpm overnight at ambient temperature to achieve a consistent clay suspension before each polymerization step. Next, various amounts of butyl methacrylate (BMA) monomer were added to the clay dispersion in a 100 mL Pyrex reaction vessel, based on the weight ratios specified in Table 1. Polymerization was initiated by introducing a benzoyl peroxide (Bz_2O_2) solution prepared in 1 mL of acetone at a concentration of 3.59×10^{-3} mol/L into the reaction mixture. The polymerization was conducted at 85 °C for 2 h using an ultrasonic bath (Bandelin Sonalex RK 100 H, Germany). Upon completion, the reaction mixture was poured into methanol to precipitate the composite material. The resulting precipitate was separated through filtration and subsequently dried in a vacuum oven at 30 °C until a stable mass was

Table 1 Composite samples and polymerization conditions[a]

Composite samples	Monomer amount (mass%)
PBMA/Na-MMT1	33.33
PBMA/Na-MMT2	50.00
PBMA/Na-MMT3	60.00
PBMA/Na-MMT4	66.67
PBMA/Na-MMT5	71.40
PBMA/Na-MMT6	75.00
PBMA/Na-MMT7	77.78
PBMA/Na-MMT8	80.00
PBMA/Na-MMT9	81.81

PBMA: poly(butyl methacrylate); Na-MMT: Na-montmorillonite

[a][Bz_2O_2]: 3.59 x 10^{-3} mol/L, temperature: 85 °C, time: 2 h

obtained. For comparison purposes, a control PBMA sample was synthesized under the same experimental conditions, excluding the presence of Na-MMT. The specific formulations and synthesis details for each composite are outlined in Table 1.

Characterization of PBMA/Na-MMT composites

All characterization data, including FTIR, XRD, TEM, FE-SEM, TGA, BET, moisture retention, water uptake, and antibacterial tests, were obtained from either pure samples or samples treated under conditions comparable to those of the composites to ensure consistent and reliable analysis. Among the composites synthesized, representative samples were selected for TEM imaging and detailed characterization evaluation because all formulations exhibited comparable structural and morphological features under identical synthesis and analysis conditions, and thus the selected samples adequately reflect the overall behavior of the series.

The sodium montmorillonite (Na-MMT) used in this study was characterized for its cation exchange capacity (CEC) using the methylene blue adsorption technique, as outlined in previous research [15]. The CEC of Na-MMT was determined to be 1.08 mol·kg^{-1}, confirming its suitability for intercalation within composite structures.

To confirm the synthesis of poly(butyl methacrylate) (PBMA) and its incorporation into the clay matrix, Fourier Transform Infrared (FTIR) spectroscopy was conducted. The spectra were recorded using a Bruker IFS 66/S spectrometer in the range of 400–4000 cm^{-1}, with samples prepared in KBr pellet form to ensure uniformity.

X-ray diffraction (XRD) analysis was employed to examine the structural characteristics of both the raw Na-MMT and the PBMA/Na-MMT composites. Measurements were taken using a Rigaku D/MAX 2200 diffractometer with CuKα radiation ($\lambda = 1.5418$ Å). Scans were performed over a 2θ range of 2° to 40° at a rate of 0.15°/min. The interlayer (basal) spacing, denoted as d_{001}, was calculated using Bragg's Law: $d = n\lambda/2\sin\theta$.

Further insight into the internal structure and dispersion of the clay layers was obtained through Transmission Electron Microscopy (TEM). For this, the composites were embedded in epoxy resin, ultrathin Sects. (70–90 nm) were cut with a Leica EM UC6 ultramicrotome, and the slices were mounted on carbon-coated 300-mesh copper grids for imaging via a FEI Tecnai G2 Spirit BioTwin TEM.

Surface morphology was observed using Field Emission Scanning Electron Microscopy (FE-SEM) with a Quanta 400 F system. Prior to imaging, sample surfaces were sputter-coated with a thin gold layer to enhance conductivity and prevent surface charging.

Thermal degradation and stability analyses of Na-MMT, pure PBMA, and composite samples were performed via Thermogravimetric Analysis (TGA) using a Perkin Elmer Pyris 1 instrument. Samples were heated from 25 °C to 800 °C under a nitrogen flow of 100 mL/min at a controlled rate of 10 °C/min.

The Brunauer–Emmett–Teller (BET) method was applied to evaluate surface area and porosity features using a Quantachrome Nova 2200 analyzer. Nitrogen adsorption–desorption isotherms were used to calculate specific surface areas and pore size distributions for both pure clay and PBMA-based composites.

Moisture retention behavior of the composites was evaluated by placing pre-dried and pelletized samples in a controlled environment at 25 °C with 100% relative humidity for 24 h. After exposure, samples were weighed, and the percentage of moisture retention was calculated using the following equation:

$$\text{Moisture retention } (\%) = [(W_2 - W_1)/W_1] \times 100 \quad (1)$$

where W_1 is the initial dry weight, and W_2 is the weight after humidity exposure [4, 17].

To assess water uptake, dried pellets were immersed in distilled water at 25 °C for 2 h. After soaking, the surface water was gently removed using filter paper, and the samples were immediately weighed. Water uptake was then calculated using the formula [4, 17]:

$$\text{Water uptake } (\%) = [(W_2 - W_1)/W_1] \times 100 \quad (2)$$

The antibacterial performance of the composites was tested using the disc diffusion method against selected Gram-negative bacteria, including *Proteus vulgaris*, *Pseudomonas aeruginosa*, and *Escherichia coli* (ATCC 35218) [18–20]. Composite discs (16 mm in diameter) were placed on nutrient agar plates that had been inoculated with standardized bacterial suspensions (0.5 McFarland standard in 0.85% saline). The plates were incubated at 37 °C for 24 h. After incubation, the inhibition zones around the discs were measured to evaluate antibacterial activity. The antibacterial effect was classified based on inhibition zone diameter as strong activity (> 13 mm), moderate activity (6–12 mm), weak activity (5 mm) or inactive (< 5 mm) [21].

Results and discussion

FTIR spectroscopy

The incorporation of Na-montmorillonite (Na-MMT) into the polymer matrix was verified using Fourier Transform Infrared (FTIR) spectroscopy. Figure 1(a–c) shows the FTIR spectra of Na-MMT, pure PBMA, and the PBMA/Na-MMT7 composite.

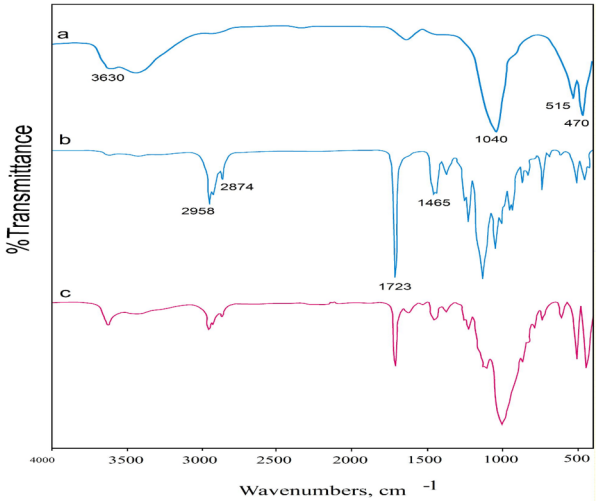


Fig. 1 FTIR spectra of **(a)** Na-MMT, **(b)** Pure PBMA, and **(c)** PBMA/Na-MMT7 composite

The characteristic absorption bands of Na-MMT were identified at 1040 cm^{-1} (Si–O–Si stretching vibrations), 515 cm^{-1} (Al–O bending), 470 cm^{-1} (Mg–O bending), and a broad O–H stretching band around 3630 cm^{-1}, attributed to structural water. In addition, a peak observed near 3400 cm^{-1} corresponds to the vibrations of adsorbed water molecules on the clay surface.

In the spectrum of pure BMA, characteristic bands were observed in the range of 2958–2874 cm^{-1}, corresponding to the C–H stretching vibrations of CH_3 and CH_2 groups. A strong absorption band at 1723 cm^{-1} was assigned to the carbonyl (C = O) stretching of the ester functional group in PBMA. In the PBMA/Na-MMT7 composite spectrum [Fig. 1(c)], this carbonyl band appeared at the same position, indicating that no significant shift occurred upon the incorporation of Na-MMT. This suggests that the chemical environment of the carbonyl groups remains largely unchanged. Furthermore, the CH_2 bending vibration band at 1465 cm^{-1} was also clearly observed in the composite spectrum.

The structural water band at 3630 cm^{-1} suggests partial penetration of the polymer into the interlayer galleries of Na-MMT, whereas the signal corresponding to adsorbed water near 3400 cm^{-1} indicates surface interactions between the clay and the polymer chains. Overall, the FTIR analysis results clearly demonstrate that Na-MMT was successfully incorporated into the PBMA matrix and that the polymer exhibits interfacial interactions with the clay, while the chemical structure of the ester carbonyl groups in PBMA remains unaffected by these interactions.

X-ray analysis (XRD)

The presence and structural integration of Na-MMT within the PBMA matrix were further verified through X-ray diffraction (XRD) analysis. The diffraction patterns of Na-MMT and PBMA/Na-MMT composites are presented in Fig. 2(a–e). The interlayer spacing values (d_{001}), representing the distance between montmorillonite

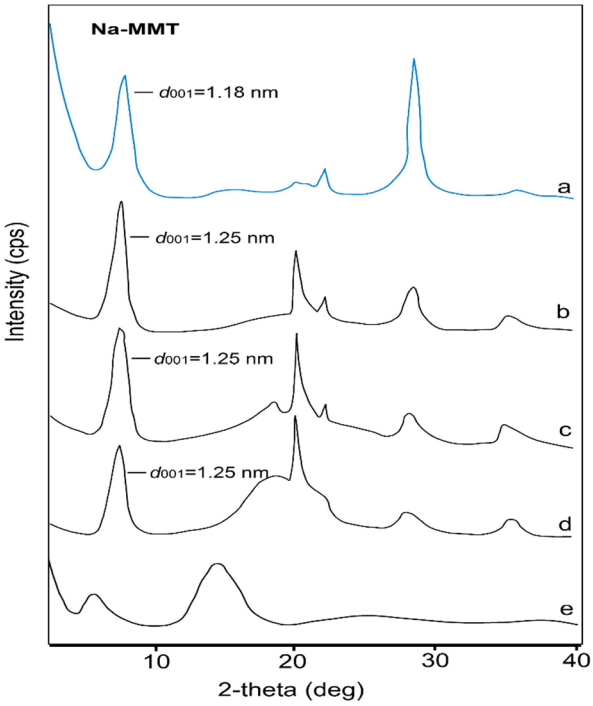


Fig. 2 The XRD patterns of **(a)** Na-MMT, **(b)** PBMA/Na-MMT4, **(c)** PBMA/Na-MMT6, **(d)** PBMA/Na-MMT8, and **(e)** Pure PBMA

layers, were determined using Bragg's equation ($d=\lambda/2\sin\theta$). Na-MMT exhibited a distinct basal reflection at $2\theta=7.46°$, corresponding to an interlayer distance of 1.18 nm, which is indicative of its well-ordered layered structure. In contrast, synthesized PBMA displayed a broad diffraction peak at $2\theta=15.86°$, characteristic of an amorphous polymer phase. Upon incorporation of PBMA into the Na-MMT structure, noticeable changes in diffraction patterns were observed. For instance, in the PBMA/Na-MMT4 composite, a shift in the basal reflection peak toward lower angles was detected, signifying an increase in the d-spacing due to polymer intercalation. The expanded interlayer distance reached 1.25 nm, suggesting successful insertion of PBMA chains between the clay layers. Similar d-spacing values were also recorded for PBMA/Na-MMT6 and PBMA/Na-MMT8, indicating consistent intercalation behavior across different compositions. The approximately 0.1 nm increase in interlayer distance highlights the structural expansion caused by polymer insertion. Furthermore, the broad amorphous phase observed in Fig. 2(e) reinforces the presence of a disordered PBMA phase in the composite materials.

Scanning electron microscopy (SEM)

To investigate the surface morphology of the synthesized composites and to evaluate the dispersion of Na-MMT layers within the polymer matrix, scanning electron microscopy (SEM) analysis was conducted. As depicted in Fig. 3(a), Na-MMT displays a stacked, plate-like, and aggregated structure prior to intercalation. How-

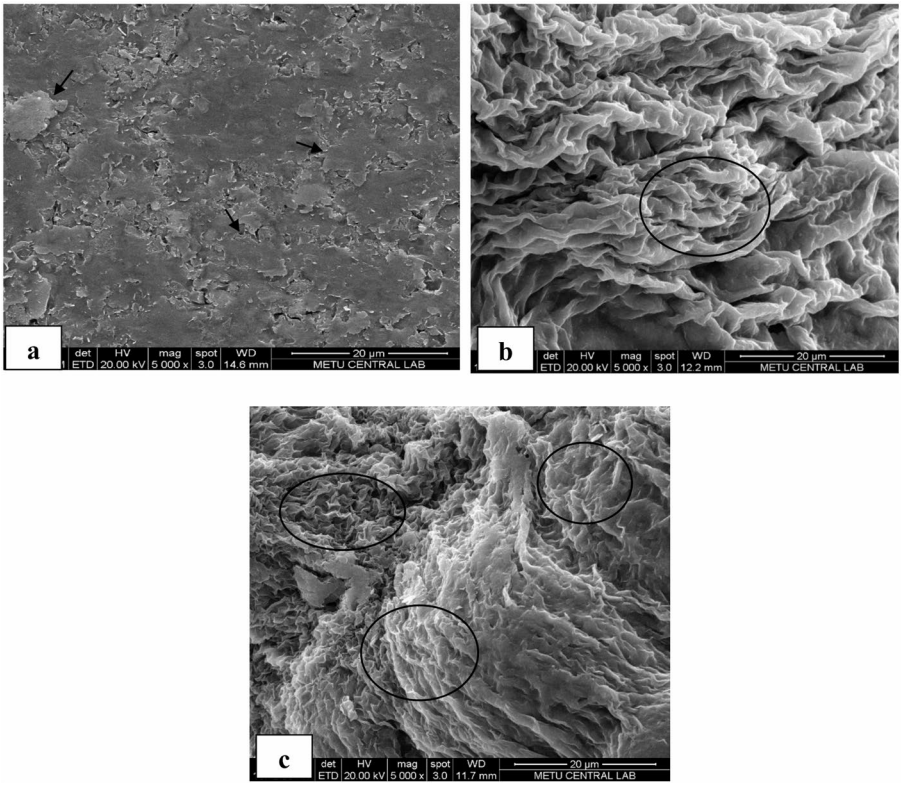


Fig. 3 SEM images of **(a)** Na-MMT, **(b)** PBMA/Na-MMT3 composite, and **(c)** PBMA/Na-MMT7 composite

ever, after intercalation with PBMA, noticeable morphological transformations are observed, as shown in Figs. 3(b) and 3(c). These changes indicate that PBMA polymerization took place between the clay layers. At increased monomer content, the resulting composite demonstrates a porous and sponge-like architecture, particularly evident in Fig. 3(c). For facilitate comparative evaluation, the corresponding morphological features are explicitly annotated in Fig. 3.

Transmission electron microscopy (TEM)

Transmission electron microscopy (TEM) was employed to assess the dispersion behavior of Na-MMT within the PBMA matrix, providing crucial nanoscale insights that complement the structural information obtained from XRD analysis. Figure 4 displays the TEM micrograph of the PBMA/Na-MMT3 composite, in which the dark fringes correspond to individual montmorillonite layers, while the brighter areas represent the polymeric matrix surrounding them. The micrograph reveals a predominantly uniform nanoscale distribution of Na-MMT layers, with clear evidence of both intercalated and exfoliated structures dispersed within the PBMA matrix. This indicates an effective level of clay dispersion, although minor agglomerations of clay

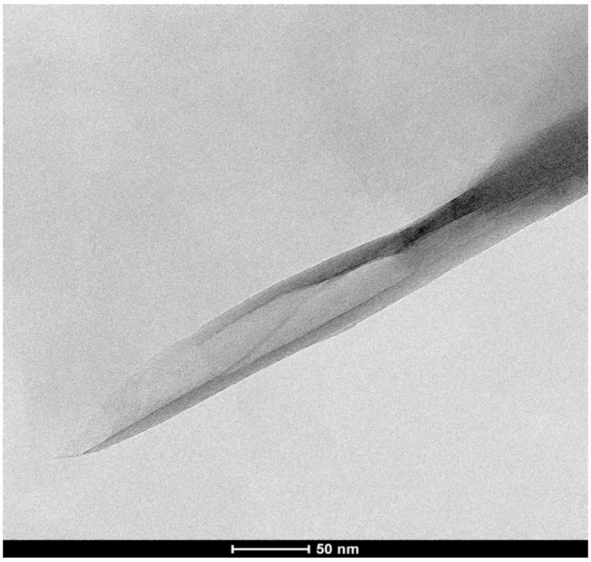


Fig. 4 TEM images of PBMA/Na-MMT3 composite

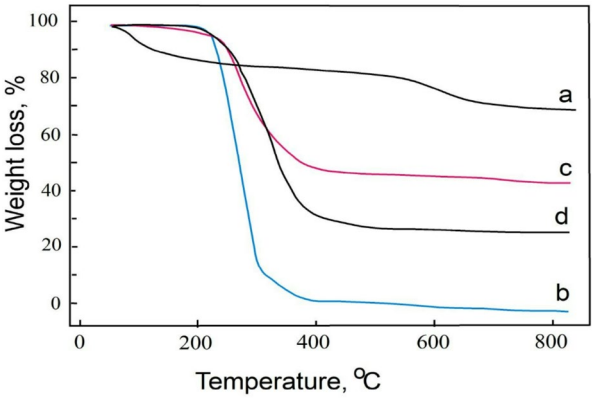


Fig. 5 TGA curves of **(a)** Na-MMT, **(b)** pure PBMA, **(c)** PBMA/Na-MMT3, and **(d)** PBMA/Na-MMT7

platelets are also visible in certain regions. As shown in Fig. 4, the composite exhibits a well-defined layered morphology, and the circled area emphasizes an intercalated domain where polymer chains penetrate between clay layers. These observations corroborate the XRD results, demonstrating consistent findings between microscopic visualization and diffraction-based analysis, and confirming that PBMA chains are successfully intercalated into the Na-MMT gaps.

Thermogravimetric analysis (TGA)

The thermogravimetric analysis results, illustrating the thermal degradation behavior of Na-MMT, pure PBMA, and PBMA/Na-MMT composites, are shown in Fig. 5(a–d). The TGA curve of Na-MMT [Fig. 5(a)] reveals two distinct stages of weight loss. The first, a minor mass reduction of about 6.13% below 125 °C, corresponds

to the evaporation of adsorbed moisture. At higher temperatures, further mass loss is observed, attributed to the dehydroxylation of the clay structure. Overall, Na-MMT exhibits a total weight loss of approximately 18.85% up to 800 °C, indicating high thermal resistance and its effectiveness as a thermal barrier [3, 4].

Figure 5(b) displays the TGA profile of pure PBMA, which undergoes a single, sharp decomposition event beginning at roughly 309 °C. This process continues to near-complete degradation (~100% mass loss) by 800 °C, reflecting the thermal decomposition of the polymer backbone and indicating lower thermal stability relative to Na-MMT.

For the composites, thermal behavior varies depending on the clay content. PBMA/Na-MMT3 demonstrates an onset of degradation at 330 °C, which is about 21 °C higher than that of the pure polymer. A minor initial mass loss of roughly 1.03% below 90 °C is attributed to the evaporation of absorbed water [Fig. 5(c)]. At 800 °C, the total weight loss is 58.08%, indicating enhanced thermal stability due to clay incorporation. On the other hand, PBMA/Na-MMT7, which contains a higher PBMA fraction (77.78 wt%), shows a slightly earlier decomposition at 325 °C and a greater overall mass loss of 77.61% [Fig. 5(d)]. The lower clay content in this sample likely reduces the thermal shielding effect. An early-stage weight loss of 3.47% below 120 °C is again associated with moisture release. Collectively, these findings confirm that incorporating Na-MMT into PBMA improves the thermal stability of the resulting composites by 16–21 °C compared to the pure polymer. This enhancement is mainly attributed to the barrier effect provided by the clay layers, which slow down heat transfer and hinder polymer chain degradation. The observed thermal behavior aligns well with previously reported literature trends [6, 16, 22].

BET surface area and micro-/mesopore volumes

The specific surface areas and micro-/mesopore volumes of Na-MMT and PBMA/Na-MMT composites were evaluated using the Brunauer–Emmett–Teller (BET) method, based on nitrogen adsorption–desorption isotherms. A detailed summary of the experimental data is provided in Table 2.

As expected, pure Na-MMT exhibited a significantly greater surface area and pore volume than the composite materials. The BET analysis revealed that Na-MMT possessed a surface area of 67.56 m^2/g and a micro-/mesopore volume of 11.10 × 10^{-2} cm^3/g. In contrast, these values were substantially reduced in the PBMA/Na-MMT composites. For example, the surface area and pore volume for PBMA/Na-MMT1 were 13.90 m^2/g and 1.46 × 10^{-2} cm^3/g, respectively; for PBMA/Na-MMT2, they measured 8.61 m^2/g and 1.28 × 10^{-2} cm^3/g; and PBMA/Na-MMT3 showed 8.17 m^2/g with a pore volume of 1.14 × 10^{-2} cm^3/g. The notable decrease in both surface area

Table 2 The BET specific surface areas (A) and specific micro-mesopore volumes (V) of Na-MMT and PBMA/Na-MMT composites

Sample	(A), m^2g^{-1}	(V)x10^2, cm^3g^{-1}
Na-MMT	67.56	11.10
PBMA/Na-MMT1	13.90	1.46
PBMA/Na-MMT2	8.61	1.28
PBMA/Na-MMT3	8.17	1.14

PBMA: poly(butyl methacrylate); Na-MMT: Na-montmorillonite

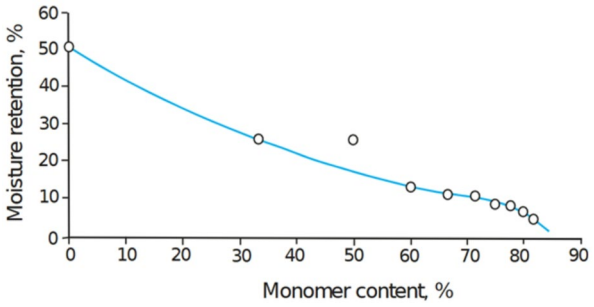


Fig. 6 Percentage moisture retention values of Na-MMT and PBMA/Na-MMT composites obtained including different percentages butyl methacrylate

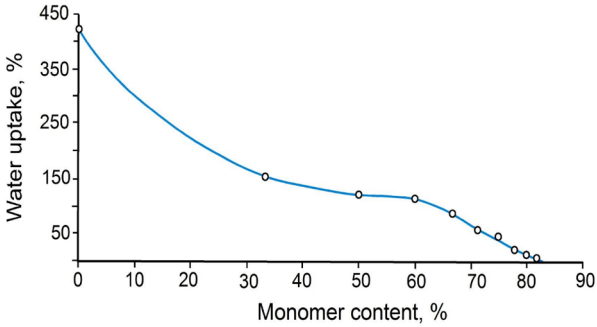


Fig. 7 Percentage water uptake values of Na-MMT and PBMA/Na-MMT composites obtained including different percentages butyl methacrylate

and pore volume across the composite samples suggests that the polymer matrix infiltrates or coats the porous structure of the Na-MMT, leading to partial or complete blockage of accessible pores. These results support the hypothesis that PBMA efficiently fills or shields the internal porosity of the clay during the in situ composite formation process [4, 16].

Moisture retention and water uptake measurements

As illustrated in Figs. 6 and 7, both the moisture retention and water uptake capacities of the PBMA/Na-MMT composites declined with increasing PBMA content. While the water uptake exhibited a gradual decrease, the reduction in moisture retention was notably more pronounced. These trends suggest that higher PBMA concentrations limit the hydrophilic character of the composites, likely due to the hydrophobic nature of the polymer matrix.

The observed reductions in moisture retention and water uptake are primarily attributed to the limited clay content within the composites [4, 23]. This limitation indicates that the amount of polymer intercalated between the clay layers reaches an optimal threshold, sufficient to maximize the expansion of the interlayer spacing. At this point, a partially cross-linked structure is formed, which restricts the penetration of water molecules into the material. Consequently, the water resistance of the composites is significantly enhanced.

Table 3 Average of Inhibition zones obtained from various composites at different concentrations of PBMA[a]

Tested Bacteria	Samples	Average of the inhibition zone(mm)
Proteus vulgaris ATCC 8427 G(-)	Na-MMT	16
	PBMA/Na-MMT1	27
	PBMA/Na-MMT5	21
Pseudomonas aeruginosa ATTCC 27,853 G(-)	Na-MMT	16
	PBMA/Na-MMT1	21
	PBMA/Na-MMT5	20
Escherichia coli ATCC 35,218 G(-)	Na-MMT	16
	PBMA/Na-MMT1	-
	PBMA/Na-MMT5	21

[a] Diameter of samples is 16 mm before experiment

Determination of antibacterial properties of prepared PBMA/Na-MMT composites

The antibacterial properties of the PBMA/Na-MMT composites, synthesized via in situ polymerization, were evaluated using the disc diffusion method [4, 20, 24]. Three Gram-negative bacterial strains Proteus vulgaris, Pseudomonas aeruginosa, and Escherichia coli (35218) were used to assess the antibacterial efficacy of the composites. The disc diffusion method was con (ducted, and the resulting zones of inhibition (measured in millimeters) were determined for various composite concentrations. The inhibition zones formed by the composite samples are summarized in Table 3.

The results indicated that pure Na-MMT exhibited no significant antibacterial activity compared to the PBMA/Na-MMT composites. In contrast, all composite samples demonstrated strong antibacterial activity, with particularly notable effectiveness against P. vulgaris, as shown in Table 3.

Conclusion

In conclusion, PBMA/Na-MMT composites with varying butyl methacrylate content were successfully synthesized and characterized. An intercalated structure was confirmed through both X-ray diffraction and transmission electron microscopy (TEM) analyses. Scanning electron microscopy (SEM) revealed that increasing the butyl methacrylate content resulted in a porous and sponge-like morphology, indicating effective dispersion of silicate layers throughout the polymer matrix. The incorporation and uniform dispersion of Na-MMT within the PBMA matrix contributed to enhanced thermal stability, as evidenced by a higher decomposition temperature compared to pure PBMA. In addition, moisture retention and water absorption values decreased with increasing PBMA content, accompanied by a reduction in BET-specific surface area and pore volume. Biological evaluations demonstrated a significant improvement in the antibacterial properties of the composites, with all samples showing notable activity particularly against *Proteus vulgaris*. Overall, the incorporation of Na-MMT clay into the PBMA matrix played a key role in enhancing both the physicochemical and antibacterial properties of the resulting composites compared to

pure PBMA, offering a promising route for the development of advanced functional polymer composites.

Acknowledgements The authors gratefully acknowledge Professor Müşerref Önal for kindly providing the clay samples that were essential to this study. The composite characterization analyses were carried out at the Central Laboratory of Middle East Technical University (METU), whose support and facilities are sincerely appreciated.

Author contributions P.A. Bozkurt: Writing – review & editing, Visualization, Validation, Methodology, Investigation, Formal analysis, Data curation, Conceptualization. S.E. Dağ: Methodology, Investigation, Formal analysis, Data curation. M. Çelik: Writing – original draft, Writing – review & editing, Project administration, Validation, Methodology, Investigation, Formal analysis, Data curation. S.P. Çelik: Methodology, Formal analysis, Data curation. L. Açık: Methodology, Formal analysis, Data curation, Conceptualization.

Funding Open access funding provided by the Scientific and Technological Research Council of Türkiye (TÜBİTAK). The authors extend their appreciation to the Scientific Research Projects Coordination Unit Project Number (16L0430012), Ankara University, Ankara, Turkey.

Data availability All data generated or analyzed during this study are included in this published article.

Declarations

Competing interests The authors declare no competing interests.

Open Access This article is licensed under a Creative Commons Attribution 4.0 International License, which permits use, sharing, adaptation, distribution and reproduction in any medium or format, as long as you give appropriate credit to the original author(s) and the source, provide a link to the Creative Commons licence, and indicate if changes were made. The images or other third party material in this article are included in the article's Creative Commons licence, unless indicated otherwise in a credit line to the material. If material is not included in the article's Creative Commons licence and your intended use is not permitted by statutory regulation or exceeds the permitted use, you will need to obtain permission directly from the copyright holder. To view a copy of this licence, visit http://creativecommons.org/licenses/by/4.0/.

References

1. Zidan TA (2020) Synthesis and characterization of modified properties of poly(methyl methacrylate)/organoclay nanocomposites. Polym Compos 41:564–572. https://doi.org/10.1002/pc.25388
2. Khelifa I, Belmokhtar A, Berenguer R, Benyoucef A, Morallon E (2019) New poly(o-phenylenediamine)/modified-clay nanocomposites: a study on spectral, thermal, morphological and electrochemical characteristics. J Mol Struct 178:327–332. https://doi.org/10.1016/j.molstruc.2018.10.054
3. Massoumi B, Abbasian M, Mohammad RR, Farnudiyan HA, Jaymand M (2019) Polystyrene-modified Novolac epoxy resin/claynanocomposite: synthesis, and characterization. Polym Adv Technol 30:1484–1492. https://doi.org/10.1002/pat.4580
4. Koç Z, Çelik M, Önal M, Sarıkaya Y, Öner Y, Açık L (2014) Study on the synthesis and properties of polyacrylamide/Na-montmorillonite nanocomposites. J Compos Mater 48:439–446. https://doi.org/10.1177/0021998312473860
5. Abass MR, EL-Masry EH, Ibrahim AB (2021) Preparation, characterization, and applications of polyacrylonitrile/ball clay nanocomposite synthesized by gamma radiation. Environ Geochem Health 43:3169–3188. https://doi.org/10.1007/s10653-021-00813-5

6. Perez RC, Vargas MLH, Cedillo OF, Illanes BFC (2019) Effect on thermo-mechanical properties by in-situ emulsion polymerization of polymer/clay nanocomposites. Polym Compos 40:263–276. https://doi.org/10.1002/pc.24640
7. Reit M, Lu X, Zarges JC, Heim HP (2025) Use of machine learning methods for modelling mechanical parameters of PLA and PLA/native potato starch compound using aging data. Int Polym Process 40(1):94–109. https://doi.org/10.1515/ipp-2024-0074
8. Vergnes B (2019) Influence of processing conditions on the preparation of clay-based nanocomposites by twin-screw extrusion. Int Polym Process 34(5):482–501. https://doi.org/10.3139/217.3827
9. Mrah L, Meghabar R (2021) In situ polymerization of styrene. –clay Nanocomposites their Prop Polym Bull 78(7):3509–3526
10. Zhu Y, Cardinaels R, Mewis J, Moldenaers P (2009) Rheological properties of PDMS/clay nanocomposites and their sensitivity to microstructure. Rheol Acta 48:1049–1058. https://doi.org/10.1007/s00397-009-0387-3
11. Vermant J, Ceccia S, Dolgovskij MK, Maffettone PL, Macosko CW (2007) Quantifying dispersion of layered nanocomposites via melt rheology. J Rheol 51:429–450. https://doi.org/10.1122/1.2516399
12. Herrera AJM, Sedlakova Z, Marand E (2010) Gas barrier properties of nanocomposites based on in situ polymerized poly(n-butyl methacrylate) in the presence of surface modified montmorillonite. J Membrane Sci 349:251–257. https://doi.org/10.1016/j.memsci.2009.11.057
13. Trivedi J, Bhatt T, Trivedi H (2014) Synthesis and characterization of poly(butyl methacrylate) grafted sodium salt of partially carboxymethylated Guar gum. Cellul Chem Technol 48:503–514 Web of Science Id WOS:000343076300010
14. Briesenick D, Bremser W (2015) Synthesis of polyamide-imide-montmorillonite-nanocomposites via new approach of in situ polymerization and solvent casting. Prog Org Coat 82:26–32. https://doi.org/10.1016/j.porgcoat.2015.01.013
15. Önal M, Sarıkaya Y, Alemdaroğlu T, Bozdoğan I (2003) Isolation and characterization of a smectite as a micro-mesoporous material from a bentonite. Turk J Chem 27:683–694. https://journals.tubitak.gov.tr/chem/vol27/iss6/3
16. Eser N, Önal M, Çelik M, Pekdemir AD, Sarıkaya Y (2020) Preparation and characterization of polymethacrylamide/halloysite composites. Polym Compos 41:893–899. https://doi.org/10.1002/pc.25420
17. Çelik M, Saçak M (1996) Grafting of methacrylic acid onto poly(ethylene terephthalate) fibers using Azobisisobutyronitrile. J Macromol Sci Pure Appl Chem 33:191–202. https://doi.org/10.1080/10601329608010862
18. Ramesh E, Manian RDRS, Raghunathan R (2009) Synthesis and antibacterial property of quinolines with potent DNA gyrase activity. Bioorg Med Chem 17(2):660–666. https://doi.org/10.1016/j.bmc.2008.11.058
19. Morsi RE, Labena A, Khamis EA (2016) Core/shell (ZnO/polyacrylamide) nanocomposite: In-situ emulsion polymerization, corrosion inhibition, anti-microbial and anti-biofilm characteristics. J Taiwan Inst Chem Eng 63:512–522. https://doi.org/10.1016/j.jtice.2016.03.037
20. Çelik M, Qudrat ML, Akyüz E, Açık L (2012) Synthesis and characterization of acrylic fibers-g-polyacrylamide. Fibers Polym 13:145–152. https://doi.org/10.1007/s12221-012-0145-5
21. Ghaffari MM, Eslani H (2014) Synthesis, characterization and antibacterial properties of a novel nanocomposite based on polyaniline/polyvinyl alcohol/Ag. Arab J Chem 7:846–855. https://doi.org/10.1016/j.arabjc.2013.11.011
22. Paul PK, Hussain SA, Bhattacharjee D (2013) Preparation of polystyrene-clay nanocomposite by solution intercalation technique. Bull Mater Sci 36:361–366. https://doi.org/10.1007/s12034-013-0498-4
23. Eser N, Önal M, Çelik M, Pekdemir AD, Sarıkaya Y (2020) Synthesis, characterization and some physicochemical properties of polypyrrole/halloysite composites. J Macromol Sci Pure Appl Chem 57:222–228. https://doi.org/10.1080/10601325.2019.1691447
24. Dag SE, Bozkurt PA, Acar N, Açık L, Çelik M (2018) Preparation and antibacterial properties of poly(N-hydroxymethyl acrylamide)/Na-montmorillonite composites via in situ polymerization. Malaysian J Chem 20:138–147

Publisher's note Springer Nature remains neutral with regard to jurisdictional claims in published maps and institutional affiliations.

Authors and Affiliations

Pınar Acar Bozkurt[1] · Sibel Erol Dağ[2] · Meltem Çelik[1] · Süheyla Pınar Çelik[3] · Leyla Açık[3]

✉ Pınar Acar Bozkurt
p3acar@hotmail.com

[1] Department of Chemistry, Faculty of Science, Ankara University, Ankara 06100, Turkey

[2] Graduate School of Natural and Applied Sciences, Ankara University, Ankara 06100, Turkey

[3] Department of Biology, Faculty of Science, Gazi University, Ankara 06500, Turkey